Available online at www.sciencedirect.com
ScienceDirect
Journal of Power Sources 162 (2006) 1254–1264
JOURNAL OF POWER SOURCES
www.elsevier.com/locate/jpowsour

Integrated fuel processor built on autothermal reforming of gasoline: A proof-of-principle study

Aidu Qi [a,b,*], Shudong Wang [b], Guizhi Fu [b], Diyong Wu [b]

[a] *Department of Chemistry and Chemical Engineering, Royal Military College of Canada, PO Box 17000, Station Forces, Kingston, Ontario, Canada K7K 7B4*

[b] *Department of Environmental and Energy Engineering, Dalian Institute of Chemical Physics, Dalian 116023, PR China*

Received 29 June 2006; received in revised form 27 July 2006; accepted 27 July 2006
Available online 24 August 2006

Abstract

One stand-alone integrated fuel processor, which not only incorporated three reaction zones, i.e., an autothermal reformer, a high temperature water gas shift (WGS) reactor and a low temperature WGS reactor, but also thermally coupled with embedded heat exchangers was developed and tested at a 1 kW scale using commercial gasoline and its surrogate *n*-octane as a hydrogen generator for fuel cell application. Mass and heat management was explored to obtain optimized temperature profiles for individual reaction zones and maximize hydrogen productivity by ensuring complete reforming of hydrocarbons, resolving the trade-off between the enhanced kinetics and the undesirable thermodynamic disadvantage of WGS reaction at high temperatures, and above all recuperating residual heat to realize higher thermal efficiency systematically. The comprehensive effect of some important independent variables on temperature profiles, hydrogen yield and CO purification were investigated, including O_2/C and H_2O/C molar ratios, fuel types and their throughput, and water allocation. A hydrogen yield of 1.5 mol-H_2 mol-C^{-1} was obtained using octane as source fuel, whereas only 1.1 mol-H_2 mol-C^{-1} for commercial gasoline. Further abatement of CO under 1000 ppm was carried out in a preferential oxidation reactor in tandem with the fuel processor. Additionally, measures on improving the fuel processor performance were put forward.

Keywords: Hydrogen; Autothermal reforming; Mass and heat management; Fuel processor; PEMFC; Distributed power system

1. Introduction

Hydrogen is widely perceived as an ideal energy carrier for a clean and sustainable energy future in the world. Fuel cells are playing a significant role on the hydrogen economy as flexible and efficient energy conversion devices [1]. To date, it seems more practical and promising to produce hydrogen on-site, which could thereby avoid the formidable issues associated with hydrogen infrastructure, transportation and storage. Recently much research and development attention has been received for autothermal reforming (ATR) of petroleum-based fuels to produce H_2 for small/medium-scale fuel cell distributed/residential power systems or auxiliary power unit (APU) applications due to their high power density, existing infrastructure of transportation and extensively public acceptability, in spite of the relatively low H_2 concentration in ATR system [2].

ATR, a combination of steam reforming (SR) and catalytic partial oxidation (CPO) reactions, offers many advantages that are not readily available in either reaction for producing hydrogen/syngas from the economic and technical point of view [3]. So far, approaches to establish hydrocarbon-based fuel processor were quite well-documented, from the perspective of both thermodynamic analysis [4–8] and dynamic investigation [9,10] as well as system optimization and process intensification, in an attempt to maximize hydrogen productivity through optimizing hydrocarbon types, reforming processes, operation conditions and catalyst/reactor designs [11–14].

In a fully integrated and efficient fuel processor, effective catalysts and reforming process/processor design are two equally indispensable, physical aspects to make it commercialized. Without doubt, it is crucial to develop catalysts suitable for ATR [15], sulfur scrubber, water gas shift (WGS) and preferential oxi-

* Corresponding author at: Department of Chemistry and Chemical Engineering, Royal Military College of Canada, PO Box 17000, Station Forces, Kingston, Ontario, Canada K7K 7B4. Tel.: +1 613 541 6000x6980; fax: +1 613 542 9489.
E-mail address: aidu.qi@rmc.ca (A. Qi).

0378-7753/$ – see front matter © 2006 Elsevier B.V. All rights reserved.
doi:10.1016/j.jpowsour.2006.07.066

dation (PROX) although this is beyond the scope of this paper. So far, much work was devoted to design and manufacture of fuel processors with a variety of compactness and integration based on different fuel processing technologies. It should be noted that parallel to the R&D of autothermal reformer, great achievement has been obtained for steam reformer plus external combustor/burner because of its unique advantages [16–19]. Nevertheless, only the R&D of efficient, compact autothermal reformer was reviewed here.

Ahmed et al. [20] proposed an annular design (not necessarily cylindrical in shape) integrated reformer using either pellet catalyst or monolithic catalyst, claiming that of the three reforming processes, ATR was most attractive as a result of its potential for higher energy efficiency, compactness and rapid dynamic response compared to other processes. This reformer was composed of several reforming zones, a sulfur removal zone (optional), multi-stage WGS and PROX (optional) zones. It also comprised of several cooling zones for reformate stream and heating zones for reactants (fuel, steam and air). Extra units such as an ignition source and a nozzle-spraying system for fuels (diesel particularly) were also possibly included. This design could help achieve high efficiencies by making good use of the 'waste energy' and decreasing heat loss from the hotspot areas, although it was in general difficult to scale-up.

By contrast, a cylindrical reactor/radial reactor with a nominally similar configuration to the annular design discussed above was developed by Bentley et al. so as to lower pressure drop through catalyst beds, reduce parasitic requirements of the reactor as well as increase the throughput [21]. It included four reaction zones and a product gas collection space, placed sequentially in space adjacent to each other. A flow path was provided for directing flow of a reaction stream in diverging directions from the 1st zone (partial oxidation) into the 2nd zone (SR), and continuing in the same diverging directions through the 2nd zone, followed by the 3rd (high temperature WGS) and 4th zones (low temperature WGS).

A more concise design was GM and Toyota's serpentine reformer [22]. It includes a mixer/evaporator, 1–2 sections for ATR and WGS each, 3–4 sections of PROX, and at least one section of combustor which were arranged sequentially in space. Similar work was carried out by Severin et al. [23]. Unfortunately, this kind of configuration needs large amount of insulation for processor integration.

The recently developed oxygen ion transportable membrane (ITM) assisted ATR was more promising [24]. First of all, N_2 dilution in the hydrogen-rich stream was avoided; secondly, the controlled supply of pure O_2 into the oxygen ITM reformer could help avoid fuel and O_2 premixing before the occurrence of reaction, eliminating NO*x* emissions and N_2 removal downstream otherwise; thirdly, it could help finely control temperature profile so as to lower the requirement for refractory material for both catalysts and reformers.

In all these proposed reformers, the efficacy of mass and energy management is essential. Note that it is only a vain attempt to study either of them unilaterally or separately taking into consideration that they are basically the two sides of the same technology, particularly when using the reactants/reformate as the heat transfer medium, i.e., recovering the residual heat from the reformate stream by the feed streams. However, it is not trivial to achieve an efficient thermal integration in fuel processors. Several schemes for heat recovery have been proposed in literatures. Burch et al. [25] proposed dividing water flow into three streams with each of them recovering the heat from different stage of the fuel processor. Similar design was also proposed and investigated by Doss et al. [26], however, relatively high operation pressures and temperatures were preferred so as to enhance the exergy of the reforming streams.

Despite all the development of various reformers, detailed work was scarce in terms of concrete reforming experiments particularly for liquid hydrocarbons such as commercial gasoline. Most importantly, the integration of fuel processor was still very limited. Moon et al. setup a fuel processing system, composed of ATR, high temperature WGS (HT-WGS) and low temperature WGS (LT-WGS) reactions, and studied their reaction behaviors, nevertheless, all the energy needed for reaction and temperature control were provided by an external furnace [27]. Sandhu et al. [28] in their numerical simulation of a *n*-decane CPO reformer for fuel cell application took PROX into account as well and studied the reformer performance as a function of catalyst loading and inlet temperatures, nevertheless, they basically studied individual units separately with little consideration of the interactions among all the units. In general, in the conventional fuel processor, extra water was directly injected/sprayed into the WGS sections as 'fire fighters' to control the temperatures and enhance the WGS reaction favorable for H_2 production [29]. In this case, water inputted locally could not be used for reforming section, which otherwise could help keep ATR temperature under control and eliminate carbon formation on catalyst surface. Another deficiency of the current studies was that several operation parameters, O_2/C ratio, H_2O/C ratio, temperatures and heat loss, which are interactive and interdependent with each other in reality, were studied respectively or discretely only, quite often resulting in biased or confused conclusions.

Therefore, with the objective of developing one stand-alone gasoline fuel processor for fuel cell application, using current catalyst suites as platform, an ATR gasoline fuel processor was designed, assembled and tested. The main goal of this paper is to study the combinatory effect of operation conditions on the ATR behavior and to have an insight into the interactive mechanisms between the operating parameters in order to further optimize the catalyst performance and eventually develop a more efficient ATR system.

2. Experimental

2.1. Experimental set-up and its schematic diagram

Fig. 1 represented the schematic diagram for the gasoline fuel processor. The main features were that it comprised of two parts, the reaction units and the embedded heat remove/recuperating units between the feeds (including fuel, air and water) and the reformate. For the reaction units, it followed the general principles of ATR fuel processors, i.e., an ATR reactor followed by high and low temperature WGS reactors. With an incen-

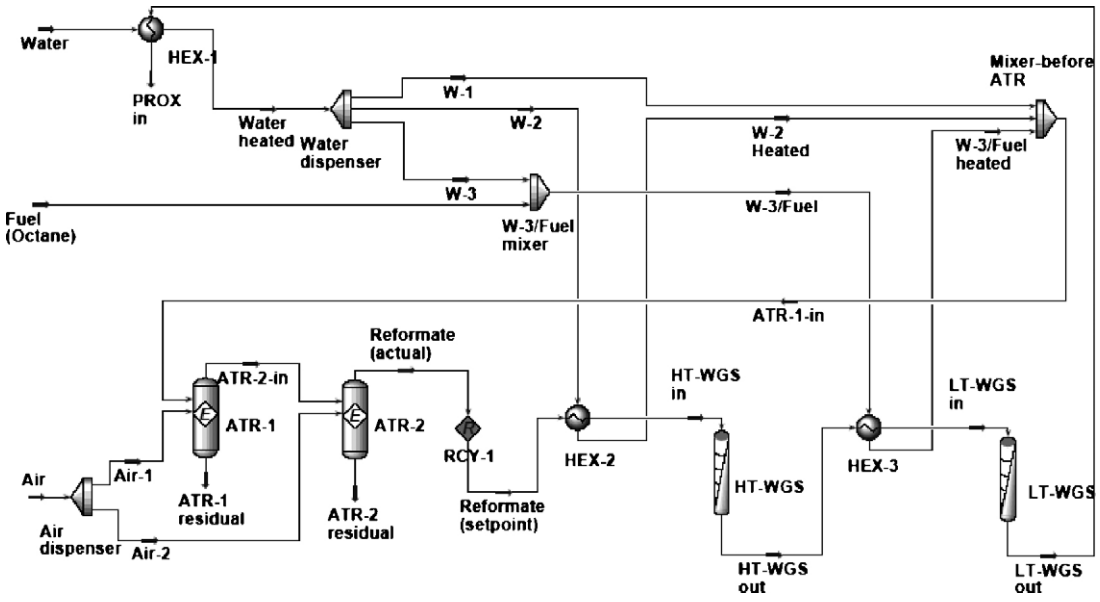

Fig. 1. Schematic diagram for the integrated fuel processor.

tive to produce PEMFC-grade hydrogen-rich stream, an external PROX reactor was in tandem so as to abate CO further (not shown in Figs. 1 and 2). During the experiment, the fuel processor was evaluated either separately or coupling with this PROX reactor. For the heat remove/recuperating units, the feeding/product channels were combined with each other to form effective heat exchangers. Water stream was divided into three parts after preliminary heating by the post LT-WGS reformate stream. The first part (W_1) was sprayed into the mixer right ahead of the ATR reformer after passing through the catalyst bed of ATR (this configuration was not embodied in Fig. 1); the second part (W_2) was to condition the reformate ready for HT-WGS before W_2 eventually merged into the ATR zone for taking part in the reforming reaction; the rest water (W_3) was used to control the inlet temperature for LT-WGS. The fuel, either octane or gasoline, combined with W_3, was fed into the mixer upstream of ATR, so its possibility of overheating was avoided. The air was introduced through the outmost layer of the reformer and eventually conducted into the ATR zone.

Based on the rationale above, a compact fuel processor similar to ANL's design [30] was fabricated. Fig. 2 demonstrated the external profile of the fuel processor and its peripherals. Clearly, the fuel processor combined the reactor, heat exchanger and even an igniter into one unit, forming a thermally self-sustaining system without external heat provision. The gross dimension was Ø150 mm × 150 mm. In Fig. 2(a), the peripherals for the fuel processor were shown including four pumps (one for fuel and the other three for water) and the air feeding system. Fig. 3 showed the detailed inside layout of the fuel processor, including the catalyst bed locations, flow patterns, thermocouple wells for the removable *k*-type thermocouples, location of the Pt filament for lighting off. Note that it is an annular design, so nearly all the designs are round and symmetric although not all of them were shown out in order to make the drawing more legible. Furthermore, although the heat exchangers in this design were based on tubing coil, it was described as modules in this figure in order to make it easy to draw and easy to understand although not necessarily clearly showing the distribution of the coils. There

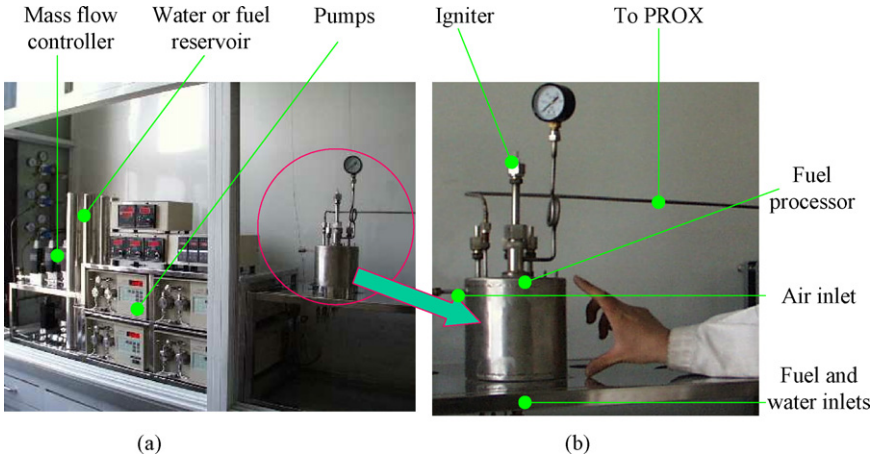

Fig. 2. Photos for the integrated fuel processor (b) and its peripherals (a).

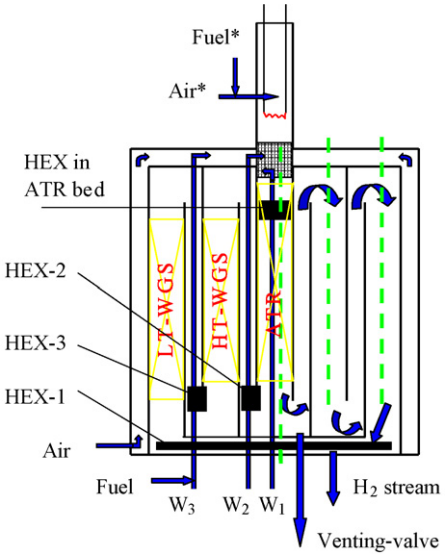

Fig. 3. Schematic diagram of the cross section of the fuel processor. (▦) Stainless steel wire; (– – –) thermocouple wells; (■) heat exchanges (HEX); (∿) Pt filament; (☒) catalyst beds; (—) reactor walls; (➡) flows; (*) alternate flow for ignition.

were special alternate routes for air and fuel near the Pt filament in order to obtain better mixture ready for lighting off and expedite the startup. Right after the lighting up, the air and fuel feeds were switched to normal operation position.

2.2. Catalysts

Corresponding to each reaction zone in this design, appropriate catalysts were either made in house or bought somewhere, which were shown in Table 1. GH12, with CeO_2 modified Ru as the main active component, was developed in house for ATR [31]. The catalyst for HT-WGS (BMC-1), mainly Fe_3O_4–Cr_2O_3, was bought from Hengyang Chemical Ltd. A commercial copper-based catalyst (B-206 bought from Sichuan Chemical Works Group Ltd.) was used for the LT-WGS reaction. Additionally, the catalyst for PROX (CO-OX-38) was produced in house. Based on the design scale of 1 kW, i.e., around 0.6–0.8 $m^3\,h^{-1}$ hydrogen was produced, the catalyst loading amount for ATR, HT-WGS, LT-WGS and PROX was 90, 400, 400 and 300 ml, respectively. All the catalysts could be either reduced on-line or require no activation prior to usage. Some other properties of the catalysts were also listed in Table 1.

2.3. Operation procedures

2.3.1. Startup

The short Pt filament was initially electrically heated for 3 s under a voltage of 5 V and a wattage of 50 W to light-off the feed mixture: gasoline/octane sprayed by air with an O_2/C molar ratio a little above the stoichiometry of full combustion. If the reaction was not started, another 3 s were repeated. Liquid fuel was supplied by pump while air was regulated by mass flow controller. The valve (called Venting-valve later) between ATR and HT-WGS reaction zones was kept open till the temperature near the entrance of ATR zone reached around 800 °C. Then the air feed was gradually decreased, accompanied by introducing water from W_1 and W_2 inlets to control the combustion temperature under 850 °C. Finally the distribution of water was finely adjusted through the whole reactor accompanied by O_2/C adjustment so as to get the predetermined temperatures (measured by movable thermocouples) for each stage. In order to avoid temperature excursion, gasoline flux could be adjusted stepwise, although the desire operation scale was around 1 kW.

2.3.2. Normal operation

When the whole system was stabilized at a desirable condition, the final H_2-rich reformate was analyzed by one HP6890 GC equipped with an active carbon column. The gas composition right after ATR, HT-WGS and LT-WGS was also analyzed through gas suction probes downstream each reacting section. The residual hydrocarbons besides CH_4, such as C_{2+} were analyzed with one Shimadz GC-13A with a capillary column. Throughout the whole system, CO was gradually converted to CO_2, producing extra amount of H_2, the yield of hydrogen (Y_{H_2}) and energy efficiency were therefore defined as follows.

$$Y_{H_2}\,(\mathrm{mol/mol\,C}) = \frac{\text{total mole amount of } H_2 \text{ in reformate stream}}{\text{total mole amount of C in feed } C_nH_m},$$

$$\text{energy efficiency}\ (\%) = \frac{\text{low heat value of } H_2 \text{ produced}}{\text{low heat value of fuel fed}} \times 100$$

2.3.3. Shutdown

The shutdown process, although it was only an auxiliary procedure in this work, was also very important. In order to avoid catalyst sintering by temperature excursion, the air feed was shut off in the first place or switched into N_2 stream. Meanwhile, the gasoline/*n*-octane flow was stopped simultaneously or right after

Table 1
Catalysts and their properties

Reaction zones	Catalysts	Developer	Main components	Operation conditions		Loading amount (ml)
				GHSV (h^{-1})	Temperature (°C)	
ATR	GH12	In house	$Ru/CeO_2/Al_2O_3$	8000 (carbon basis)	600–800	90
HT-WGS	BMC-1	Bought	Fe_3O_4–Cr_2O_3	2000	350–450	400
LT-WGS	B206	Bought	$CuO/ZnO/Al_2O_3$	2000	180–250	400
PROX	CO-OX-38	In house	Pt/Al_2O_3	4000	100–250	300

air shutting-off, followed by gradually decreasing W_1, W_2 and W_3 in sequence until the temperature through the catalyst beds below 300 °C.

3. Results and discussion

3.1. Startup and remarkable system characteristics

In a stand-alone fuel processing system for producing hydrogen, startup is critical considering that each reaction has its own optimum operation parameters, namely temperatures, throughput, feeding ratios and so on. The preferred temperature ranges for ATR, HT-WGS, LT-WGS and PROX based on current catalysts were 600–850, 350–450, 180–280 and 100–250 °C, respectively. The conventional heating up process for catalyst beds, either by hot air [23] or electrical heater [32], was time-consuming for practical usage particularly when dealing with on-board system or auxiliary power units. Above all, too much external electricity had to be consumed to reach a light-off temperature. Currently, there primarily existed two promising startup strategies, the parallel heating strategy and the sequential heating strategy. The latter method was used in our work. A complete combustion reaction in gas phase then on the ATR catalyst bed could be initiated immediately by the Pt filament, enabling a quick startup in less than 5 min, 3.5 min for reagents pre-feeding and 0.5 min for light-off included (see Fig. 4). It should be noted that in order to mitigate the negative effect of harsh temperature on the catalyst activity and durability during startup because of the possible sintering, better reactor design was needed. Initially, the flue gas was vented off via the Venting-valve till the ATR catalyst bed arrived at a temperature around 700–800 °C. This operation avoided the catalysts downstream of ATR zone were contaminated by the unconverted heavy hydrocarbons at the beginning. However, this also made the sequential heating up process a little longer. Fig. 4 showed that the catalyst beds for WGS were only slightly above room temperature when the temperature of the ATR bed arrived at 800 °C. As soon as the Venting-valve was shut off, the temperature of WGS increased sharply, and all the temperatures (the temperature of PROX was not shown here) began to level off near their predetermined temperature in around 50 min, indicating the whole system was stabilizing.

Through the whole starting-up procedure, finely tailoring the feeding flux and their molar ratios was crucial. Fig. 5 showed a typical set of molar ratios for O_2/C and H_2O/C in the operation procedure. Just as discussed above, the initial value for O_2/C was set to 2.0, above the theoretical point 1.56 for ensuring a full combustion reaction. 10–30 s later when the temperature of the ATR bed reached 800 °C, O_2/C molar ratio was decreased gradually to around 0.5–0.6, accompanied by the adjustment of the H_2O/C ratio. The initial H_2O/C was zero in spite of the possible risk of carbon formation on the ATR catalyst bed at low temperatures. Then water was introduced from W_1 inlet to keep the ATR temperature under control and tailor the temperature of HT-WGS simultaneously. Finally water streams through the three inlets were allocated to control the temperatures for all zones.

A fuel processor was a complex system. There were numerous reactions that could possibly happen although only four of them were independent. For the ATR alone, the possible reactions were as follows [33]:

$$C_8H_{18} + 12.5(O_2 + 3.76N_2) \rightarrow 8CO_2 + 9H_2O + 47N_2 \quad (1)$$

$$C_8H_{18} + 8(O_2 + 3.76N_2) \rightarrow 8CO_2 + 9H_2 + 30.08N_2 \quad (2)$$

$$C_8H_{18} + 4(O_2 + 3.76N_2) \rightarrow 8CO + 9H_2 + 15.04N_2 \quad (3)$$

$$C_8H_{18} + 3.5H_2O \rightarrow 1.75CO_2 + 6.25CH_4 \quad (4)$$

$$C_8H_{18} + 16H_2O \rightarrow 8CO_2 + 25H_2 \quad (5)$$

$$C_8H_{18} + 8H_2O \rightarrow 8CO + 17H_2 \quad (6)$$

$$C_8H_{18} + 8CO_2 \rightarrow 16CO + 9H_2 \quad (7)$$

$$CH_4 + 2H_2O \rightarrow CO_2 + 4H_2 \quad (8)$$

$$CH_4 + H_2O \rightarrow CO + 3H_2 \quad (9)$$

$$CO + H_2O \rightarrow CO_2 + H_2 \quad (10)$$

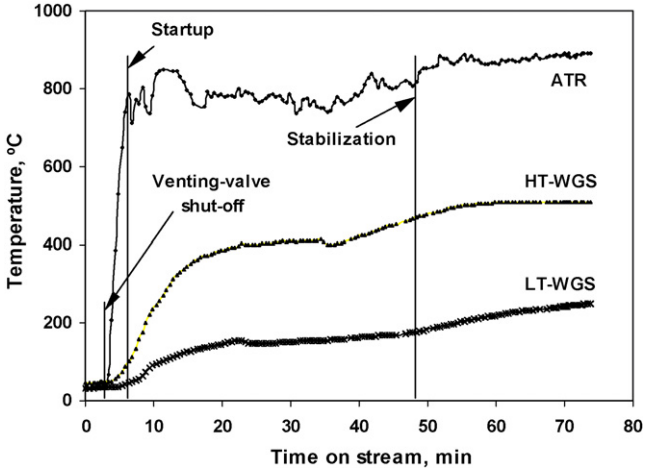

Fig. 4. Temperature profiles during startup.

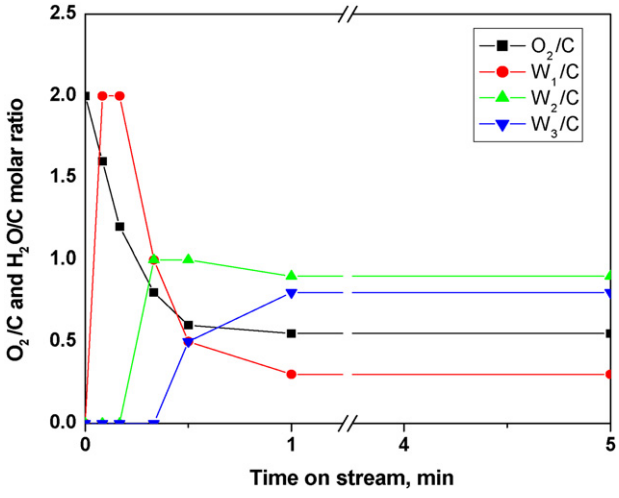

Fig. 5. Typical molar ratios for O_2/C, H_2O/C and water allocation in the operation procedure.

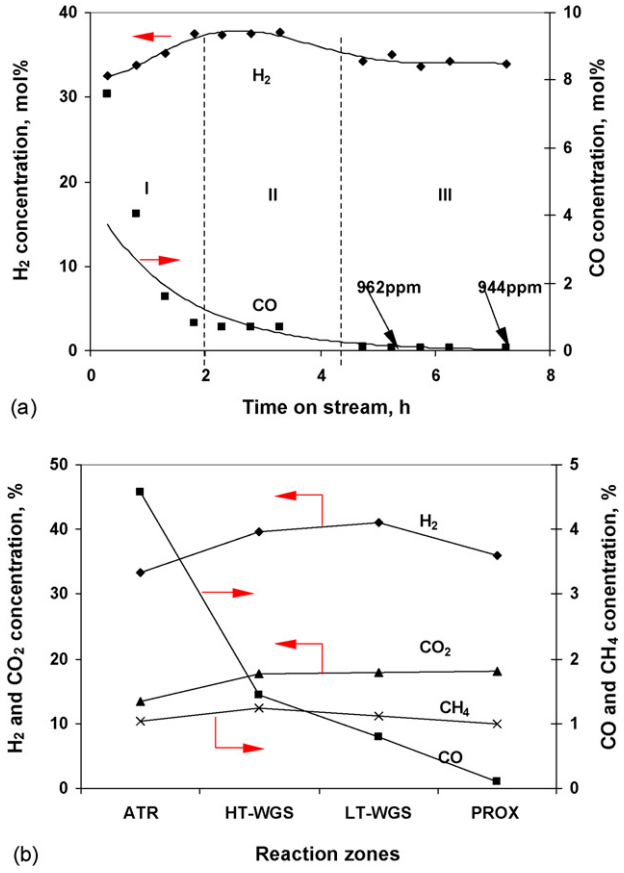

Fig. 6. Reformate concentration profile along with time during starting-up (a) and as a function of reaction zones during normal operation (b). Section I: combustion and reforming zones are stabilizing; Section II: WGS (including HT and LT) zones are stabilizing; Section III: PROX besides other zones is stabilizing;

$$CO + 3H_2 \rightarrow CH_4 + H_2O \quad (11)$$

$$CO_2 + 4H_2 \rightarrow CH_4 + 2H_2O \quad (12)$$

Although only complete combustion (Eq. (1)) was expected initially in an air-excess atmosphere, nearly all the reactions could actually happen due to the low temperature during startup. When a steady condition was reached at around 800 °C, ATR, CPO (Eq. (2)) and SR (Eqs. (5) and (6)) were predominant while the WGS (Eq. (10)) or methanation (Eqs. (11) and (12)) reactions could be either ignored or their reverse reactions were pronounced. In HT-WGS and LT-WGS zones, only WGS reaction would primarily take place to abate the CO level below 0.5–1%. CO would further be eliminated to below 1000 ppm by PROX in this work, albeit the ultimate goal was to reach PEMFC-grade H_2 stream. Fig. 6(a) showed a set of concentration profiles for H_2 and CO along with time on stream in a typical starting-up process. The startup procedure could arbitrarily be divided into three phases. In Section I (from startup to 1.5 h), ATR stage was stabilizing while WGS zones (including HT and LT ones) were not functional yet in terms of temperature, so CO produced by ATR could not fully be converted into CO_2 and produce extra hydrogen, which led to the relatively high CO and low H_2 concentrations in the stream, i.e., 9–2 and 33–35 mol%, respectively. In Section II (from 1.5 to 4 h), the whole processor (including ATR and WGS zones) was tending to be stabilized with CO and H_2 concentrations around 1 and 38 mol%, respectively. In Section III right after 4 h, air was introduced into the PROX reactor so as to initiate the CO selective reaction and suppress CO concentration to below 1000 ppm, 944–962 ppm in this work for instance.

Once the whole system was approaching to stabilization, the performance of each reaction zone was explored by the concentration checkup from the gas suction probe right after each reaction zone. As shown in Fig. 6(b), at ATR section where operation temperature was generally as high as 600–800 °C, *n*-octane was fully reformed into CO, CO_2 and H_2 although small amount of short-chain hydrocarbon, primarily CH_4 could still remain in stream. Because the reaction temperature was so high, all reactions were presumed to approach their equilibria, where Eq. (6) mainly took place to produce CO rather than Eq. (5). At HT-WGS zone, only the expected reaction of WGS was believed to happen. CO could be massively suppressed from above 4.5 to 1.5 mol% by making good use of the high WGS reaction rate at high temperature, with a hydrogen concentration increasing from around 34 to 37 mol%. CO conversion in LT-WGS zone was relatively limited compared with HT-WGS zone, nevertheless, a desirable CO level could be achieved at low temperatures with a concentration of hydrogen and CO around 38–39 and 1%, respectively. The PROX zone preliminarily purified the CO level below 1000 ppm, 944 ppm for example, however, the concentration of hydrogen suffered a lot because of the parasitic consumption as well as nitrogen dilution. Therefore, it was essential to promote CO selective oxidation reaction with as little parasitic hydrogen consumption as possible. It seemed that methods such as designing multi-stage PROX reactors [34], developing steam-resistant catalysts [35] for PROX were quite helpful. Moreover, the 'waste energy' in practice was so massive due to the parasitic hydrogen oxidation that heat recovery between PROX stages is indispensable for a higher thermal efficiency [30].

3.2. *Effect of O_2/C molar ratio at different H_2O/C molar ratios*

In a fuel processing system, there were essentially two independent variables, the O_2/C and H_2O/C molar ratios (the operation pressure and heat loss were independent but beyond this discussion). The reaction temperature, by contrast, is a dependent variable, which was controlled/adjusted by the former two. Nevertheless, temperature is the most important variable in practice taking into consideration that there always exists an optimal operation temperature point or range for the catalysts, beyond which either the catalyst has low activity/selectivity or is sintered/deactivated by various factors. There were two more independent variables among the three water allocation streams considering that temperature profiles could be finely tailored by them, which would be discussed vide post.

Theoretical analysis in our early study showed that the optimal H_2O/C in the feed was around 1.5–2.0 and the corresponding O_2/C was in between 0.35 and 0.5, where a hydrogen yield

of 1.8–2.1 mol-H_2 mol-C^{-1} could be derived [31]. However, in a real-world fuel processor, a much higher O_2/C molar ratio was required either because of the heat loss or because of larger H_2O/C molar ratio used. Note the O_2/C molar ratio here referred to the molar ratio in ATR zone only, not counting the O_2 (air) input for PROX. Fig. 7 showed hydrogen yield and ATR outlet temperature as a function of O_2/C molar ratio at various H_2O/C molar ratios. It was not surprised to find the results were of a little variation taking into consideration that, on the one hand, there usually existed thermo-kinetic oscillatory behaviors for autothermal reforming systems [36], on the other hand, the changes of O_2/C and/or H_2O/C molar ratios could result in the passive changes of temperature profile, which in turn significantly affected reaction behavior and heat/mass management. Therefore an optimum operation range other than a point could possibly be identified. Statistically, the data in this figure could be classified into two groups: the low H_2O/C (ca. 1.6–1.8) group and the high H_2O/C (ca. 2.2–2.5) group. In whichever group, the highest temperature in top ATR zone (arbitrarily called combustion zone or combustion temperature in this paper) was kept below 850 °C to protect the ATR catalyst. When the total H_2O/C was around 1.6–1.8, together with the increase of O_2/C from 0.35 to 0.5, the temperature near the combustion zone increase sharply to form a hot spot near ATR entrance, which was necessary for further SR reaction like an adiabatic reactor. However, just as shown in Fig. 7(b), the outlet temperature of ATR decreased from around 650–400 °C, which suggested an enlarged temperature drop through the ATR catalyst bed at higher O_2/C molar ratios. The massive temperature gradient through ATR catalyst bed had both advantages and disadvantages. On the one hand, it was a good indication that SR, a strongly endothermic reaction which was the main contributor to hydrogen production, took place extensively downstream of the hotspot. Thus the total hydrogen yield increased due to the increased conversion of hydrocarbon along with O_2/C increasing. Further increase of O_2/C might enhance the hydrogen productivity in principle when H_2O/C = 1.6–1.8 by deeply reforming the residual short-chain hydrocarbons, however, the maximum allowable temperature near 'hotspot', which had already reached around 850 °C when O_2/C = 0.53, was constrained by the possible catalyst sintering and even reactor collapsing. On the other hand, it was always a great goal for researchers to operate the ATR reaction with an evenly distributed temperature profile through the catalyst bed, which was also the ultimate objective of ATR reaction by carrying out both CPO and SR on one catalyst bed although not necessarily on the same active sites. In practice, the significant temperature gradient could never be avoided in that it was not easy to couple compactly the strong exothermic reaction and endothermic reaction thanks to the significant difference of reaction time scales, although GH12, a noble metal-based catalyst, had good activity for both CPO and SR [2,37]. As a result, from the catalyst configuration point of view, wall-mounted catalyst such as monolithic or microchannel catalyst was more promising [38,39]; from the reactor design point of view, reformer with multiple oxygen (air) inlets showed potential for resolving this dilemma, and reactors with embedded oxygen ITM to control oxygen feeding should be resorted to eventually.

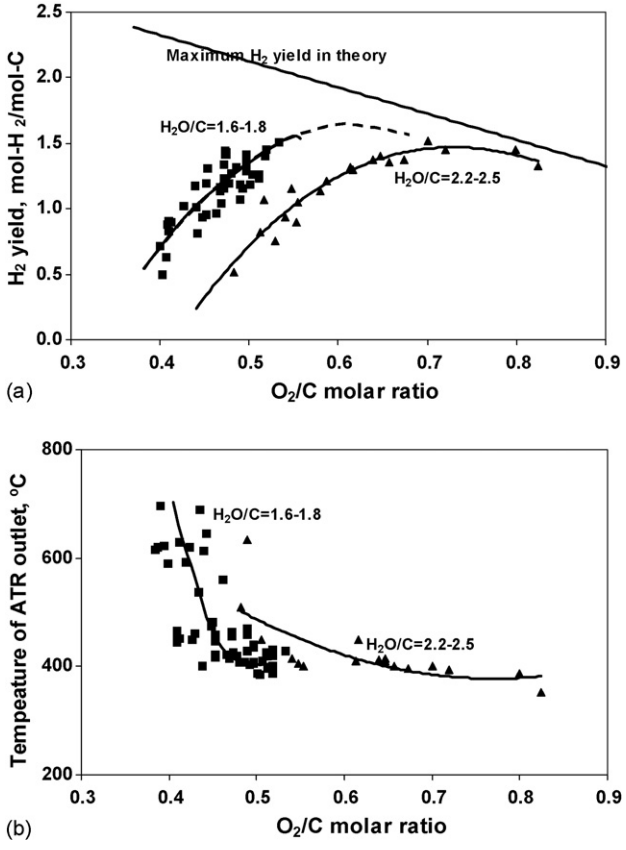

Fig. 7. Effect of O_2/C molar ratio on hydrogen yield (a) and temperature profile (b) at different H_2O/C molar ratios.

When H_2O/C molar ratios were around 2.2–2.5, higher O_2/C ratios had to be used in order to get similar operation temperatures to H_2O/C = 1.6–1.8, namely combustion reaction temperature around 800–850 °C and ATR catalyst outlet temperature around 400–600 °C (Fig. 7(b)), indicating a more energy-intensive process. This was due to the fact that more heat was used to preheat and evaporate the excess water to a desired temperature. Furthermore, deep reforming of short-chain hydrocarbons, as a strong endothermic reaction, could be strongly promoted with the existence of more steam produced at higher O_2/C in addition to the already increased H_2O/C in the feed. However, there existed a trade-off as well. On the one hand, hydrogen yield was indeed increasing because both hydrogen extraction from hydrocarbons and WGS reaction were enhanced by excess amount of steam; on the other hand, the maximum hydrogen productivity was greatly compromised due to the increased fuel consumption by oxidation reaction. Even worse, the hydrogen concentration was heavily diluted by N_2, which would finally devastate the operation of the fuel cell if applicable. At H_2O/C = 2.2–2.5, hydrogen yield reached its acme, around 1.4 mol-H_2 mol-C^{-1} for octane at O_2/C = 0.65. Further increasing oxygen flux could only result in hydrogen yield loss (Fig. 7(a)). Meanwhile, it was reasonable to presume there existed an optimum hydrogen yield for the scenario of H_2O/C = 1.6–1.8 provided better refractory materials were used

although the peak hydrogen production was shifted towards lower O_2/C molar ratios. It should be mentioned that the maximum hydrogen production for both cases were all far below the maximum possible value in theory because of the heat loss of the whole system which would be discussed below.

3.3. Effect of water distributions

Just as described above, fuels were always introduced from W_3 inlet to avoid decomposition prior to mixing with O_2 and steam. Air was always fed through the external channel around the whole fuel processor to minimize heat loss from the system as a special insulation layer. In this case, the temperature profile and reaction extensiveness were mainly tailored by water distributions through the fuel processor, and vice versa. In another word, water allocation played a great role on controlling temperatures for all zones particularly WGS zones. Moreover, the final convergence of the entire separate water streams was significantly beneficial for ATR reaction application, compared with the conventional design, in which water was sprayed right into each section only as 'fire fighters'.

There existed a well-known trade-off for WGS reaction: at high temperature, reaction rates were high at a cost of low CO conversion; at low temperature, low CO equilibrium concentration could possibly be reached however at the expense of low CO converting rate and more catalyst usage [23]. In this fuel processor, desired inlet temperatures for both HT-WGS and LT-WGS were obtained by a comprehensive water management so as to make good use of the high reaction rate in HT-WGS and better equilibrium CO conversion in LT-WGS. It should also be noted that water allocation could simultaneously affect the ATR inlet temperature due to different 'waste heat' recovery, which made the operation even more complicated.

The total H_2O/C (around 2.0–2.1) and O_2/C (ca. 0.55) molar ratios were fixed roughly in this study. Fig. 8 demonstrated the effect of water distribution on the hydrogen yield (a), the corresponding water allocation for W_1 and W_3 (b), and temperature profiles (c) in each zone. Likewise, the experiment result was of a little fluctuation resulting from the fact that the change of water allocation could cause the corresponding adjustment of various parameters.

Along with the increase in the W_2 (the stream right ahead of HT-WGS) with a W_2/C ranging from 0 to 1.7, W_1 (through ATR bed) and W_3 (the stream between HT-and LT-WGS) had to correspondingly decrease to get the predetermined operation temperatures, with W_1/C and W_3/C ranging from about 1.6 to 0.2 and from about 0.6 to 0.05 (Fig. 8(b)). Clearly, W_1 and W_2 not only accounted for the largest percentage of water stream but the biggest changes as well, indicating the importance of mass/energy management upstream of HT-WGS. With W_2/C from 0 to 1.0, combustion temperature as well as the ATR outlet temperature increased a little not only because of the effective heat recuperating from reformate, but also because of less cold water (W_1) entering ATR bed which enabled a relatively higher average temperature for ATR catalyst bed and therefore a more complete reforming reaction of hydrocarbon to produce permanent gases (H_2, CO and CO_2). Meanwhile, the slightly increased

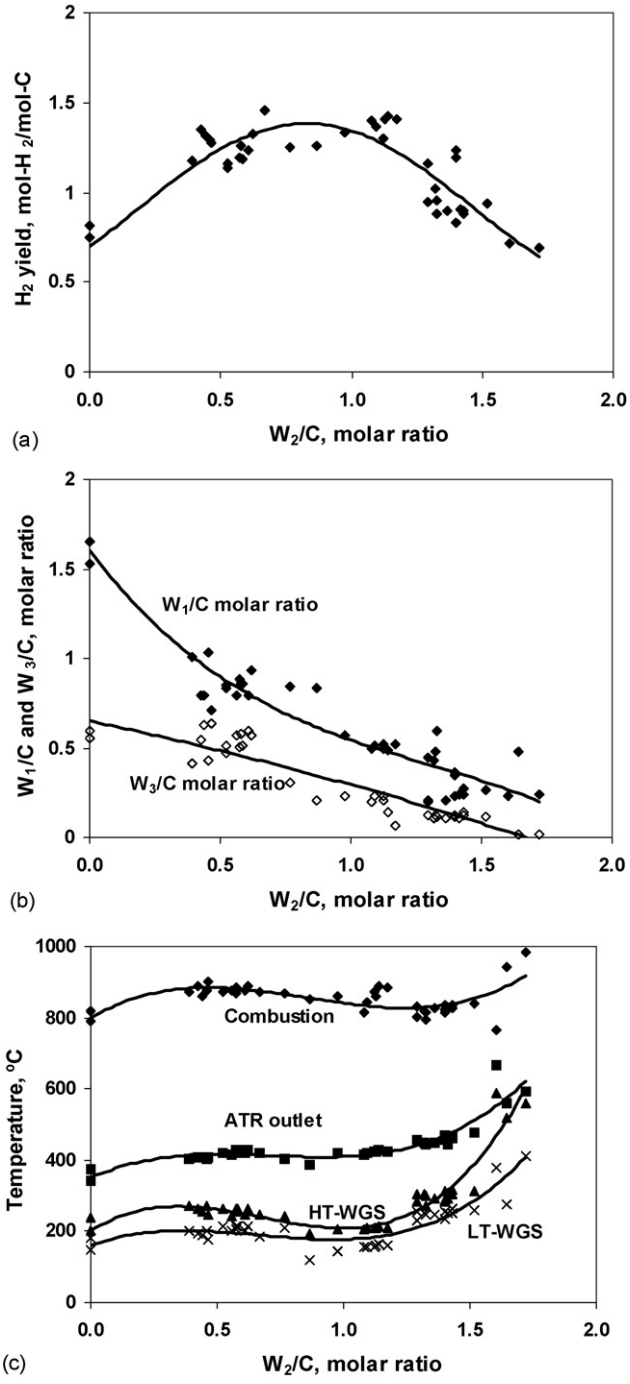

Fig. 8. Effect of W_2 on hydrogen yield (a), the balance of the other two streams (b) and temperature profiles (c).

inlet temperature for HT-WGS and the low temperature for LT-WGS (Fig. 8(c)), also as a direct result of the increased W_2/C, could synergetically form a favorable temperature profile for WGS reaction. Hence, hydrogen yield reached its peak value at W_2/C of 1.0 (Fig. 8(a)).

However, further increasing W_2/C deadly threatened hydrogen production and resulted in hydrogen yield downwards. On the one hand, the overabundant water from W_2 was not able to be fully evaporated and mixed with other reactants, which eventually devastated the ATR reaction due to the limited inlet

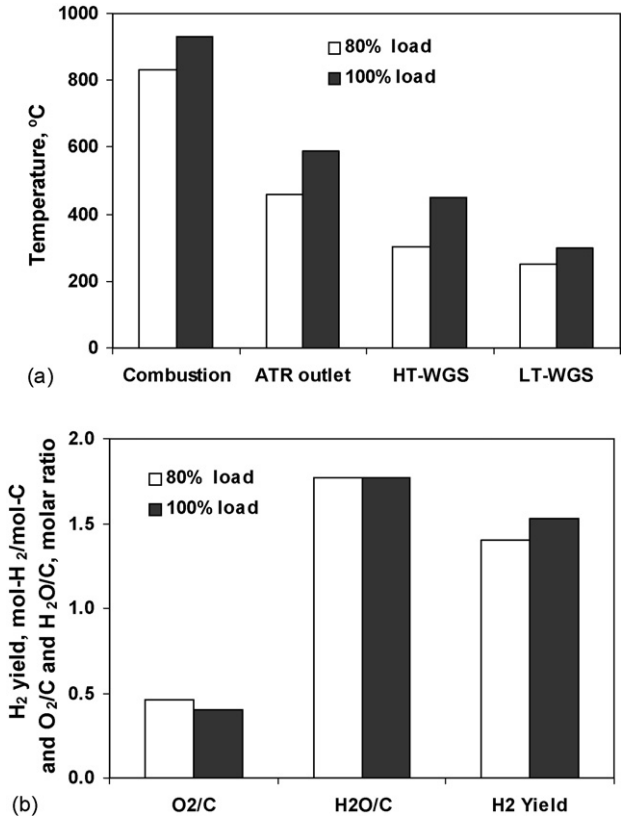

Fig. 9. Effect of the loading scales on operation parameters and hydrogen yield: (a) temperatures and (b) O_2/C and H_2O/C molar ratios and hydrogen yield.

(premixing) temperature. As such, locally favorable combustion reaction and poor steam reforming accounted for the temperature shoot-up to 1000 °C when W_2/C = 1.7 (Fig. 8(c)). On the other hand, unfavorable temperatures for HT-WGS and LT-WGS were obtained when W_2/C was above 1.0. The catalyst for HT-WGS quickly lost its expected function either because of the poor equilibrium conversion or the catalyst deactivation at high temperatures. Meanwhile, copper-based catalysts were much more vulnerable to high temperature atmosphere. Accordingly, hydrogen yield sharply decreased from 1.4 to 0.6 mol-H_2 mol-C^{-1} right after W_2/C = 1.0. Preliminary study showed that the optimum water distribution for W_1, W_2 and W_3 were around 20–30, 40-60 and 20–30%, respectively. In order to expedite an automated and turnkey fuel processor, a comprehensive numerical simulation was highly needed so as to optimize the water distribution or establish the algorithm among all the streams.

3.4. Effect of heat loss at different processing scales

The fuel processor was operated at two scales, 100% load (1 kW) and 80% load (0.8 kW). Fig. 9 showed the comparison between them. It was of interest to find that all temperatures at different stages when running the processor at a full scale (i.e., 1 kW) were slightly higher than that when operating it at an 80% scale (Fig. 9(a)) although the actual O_2/C molar ratio for the latter was on the contrary a little bigger than the former at roughly the same H_2O/C molar ratio of 1.8 (Fig. 9(b)). The hydrogen yield for the full-scale case was around 1.6 mol H_2 mol-C^{-1} whereas for the 80% loading case only 1.45 mol H_2 mol-C^{-1}. Caners [40] also found that a higher flowrate of *iso*-octane would increase the hydrogen output percentages, and the corresponding O_2/C molar ratio needed tended to become lower when he studied the *iso*-octane ATR in a compact ATR gasoline reformer for fuel cell application.

There might be several factors that accounted for this result, among which the heat loss from the system to the surroundings were a most important one. Empirically, the net heat loss by the whole system remained essentially the same in absolute terms for different operation scales considering that the temperature difference between the system and the ambient were within a certain range and the gross surface areas of the reactor was kept constant. Therefore, when operating the reactor at a higher throughput, the heat loss to the overall input energy represented a relatively smaller percentage. This was indirectly verified by the fact that the gross hydrogen yield and hydrogen concentration could increase slightly when better insulation was applied for preventing heat loss. This reforming scale-reliant phenomenon for system efficiency was also discussed by Lee et al. [32] in their studies of natural gas reforming in an integrated fuel processor and in Argonne National Laboratory's 4 kW reformer [41].

3.5. Preliminary reforming on commercial gasoline

The ultimate goal of a fuel processor was to use commercial gasoline as the source fuel. However, the additives in commercial gasoline profoundly affect the performance of ATR catalysts let alone the existence of sulfur compounds, which could strongly inhibit or poison the current ATR catalysts, including precious metal-based catalysts. The existence of sulfur could further affect the downstream catalysts and corrode the reactors. Furthermore, in a fully integrated fuel processor, the deteriorated performance downstream of ATR could in turn affect the performance of ATR from both the reaction aspect and the management of heat and mass.

In our experiment, GH12 for ATR had strong endurance to sulfur and could convert sulfur compound into hydrogen sulfide, whereas catalysts for HT-WGS and LT-WGS were very susceptible to sulfur poisoning. It was an effective way to adsorb H_2S using ZnO as a sulfur scrubber between ATR and HT-WGS zones. Alternatively, deep sulfur removal from the source-fuel has nowadays shown strong potential for desulfurization from the very beginning of the fuel processing system [42].

Fig. 10 showed the performance of fuel processor using commercial gasoline (simulated formula $C_{7.3}H_{14.8}O_{0.1}$) with ~127 ppmw sulfur as the source fuel. As soon as the fuel processor run steadily using an *n*-octane feeding rate of 305 ml h^{-1}, O_2/C = 0.4, H_2O/C = 2.0, gasoline was introduced into the fuel processor at the identical operation conditions. It was found that the combustion temperature would stabilize at a relatively higher level, however, the HT-WGS temperature almost kept unchanged while the temperature of LT-WGS slightly decreased instead (Fig. 10(a)). The multi-fuel property of gasoline and the existence of sulfur were presumed to account for these phe-

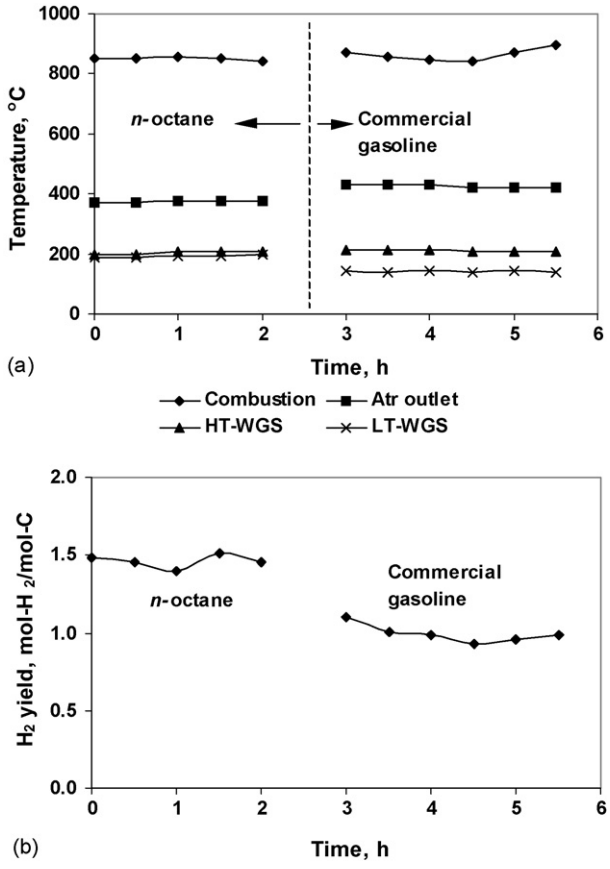

Fig. 10. The comparison between *n*-octane and commercial gasoline reforming behaviors: (a) temperature profiles and (b) hydrogen yield.

nomena although there were probably many other contributing factors. It seemed that the components with low ignition point were prone to start the combustion reaction in both gas phase and on the catalyst bed, which led to the higher combustion temperature. Meanwhile, the slow reforming reaction for hydrocarbons like aromatics with strong π-chemical bonds led to a smaller temperature gradient in ATR zone. In contrast, the HT-WGS reaction changed very little in our experiment, whereas copper-based catalyst for LT-WGS basically lost their activity instantly because of the trace amount of sulfur (ca. 1–5 ppmw hydrogen sulfide in stream after reaction), therefore the temperature for them either almost kept stable or slightly decreased.

Table 2 showed the comparison of 1 kW fuel processor in this work (based on both *n*-octane and gasoline) with a DOE 4 kW fuel processor [41]. Only a ∼1.1 mol-H_2 mol-C^{-1} for gasoline and ∼1.5 mol-H_2 mol-C^{-1} for octane could be achieved at an O_2/C molar ratio of 0.45, although a theoretical analysis showed that maximum hydrogen yield for gasoline and *n*-octane were 1.8 and 2.2 mol-H_2 mol-C^{-1}, respectively, at a O_2/C molar ratio of 0.38. Therefore, it seemed that the hydrogen yield difference between gasoline and octane was quite similar to the theoretical difference, all around 0.4–0.5 mol-H_2 mol-C^{-1}. As a result, it was reasonable to believe the hydrogen yield difference between commercial gasoline and octane was mainly resulted from the source fuels. Table 2 also showed that a H_2 concentration of 32–34 mol% and a gross energy efficiency of

Table 2
A comparison of 1 kW fuel processor in this work with a 4 kW fuel processor in literatures

Scales[a]	1 kW		4 kW
Fuels	Octane	Commercial gasoline	Synthesized hydrocarbons
Reformate (mol%)			
H_2	37–38	32–34	∼40
CO	0.6–1.2	0.6–1.5	∼2
H_2 yield (mol mol-C^{-1})	1.5 (2.2 maximum)	1.1 (1.8 maximum)	–
Efficiency (%)	68–70	62–65	75
Power density (kW l^{-1})	0.4	0.3	0.57

[a] Without CO PROX.

62–65% were obtained for gasoline, whereas a H_2 concentration of 37–38 mol% and an energy efficiency of 68–70% for its substitute octane. This result was only slightly below the level of DOE's reformer in terms of hydrogen concentration and energy efficiency. It should be mentioned that the power densities were very small, only around 0.3–0.4 kW l^{-1} for this fuel processor and 0.57 kW l^{-1} for the ANL's. To substantially improve the power density, more efficient WGS catalysts, particularly medium-temperature WGS catalysts were highly needed [43] considering that the volume ratio between WGS catalysts and ATR ones was more than 6 in the current fuel processors.

4. Conclusions

One conceptual integrated fuel processor was designed, setup and run for about 85 h at a 1 kW scale. It could startup in less than 5 min and be stabilized in around 50 min for the whole system. By adjusting the O_2/C, H_2O/C molar ratios and water distribution synergistically, optimized temperature bands for reaction zones (including ATR, HT- and LT-WGS) were achieved, and a hydrogen yield of 1.5 mol-H_2 mol-C^{-1} for *n*-octane and 1.1 mol-H_2 mol-C^{-1} for gasoline was obtained, with corresponding hydrogen concentration of 37–39 and 32–34 mol%, respectively. However, the hydrogen yield was far below the theoretical value because of the heat loss, particularly at a lower operation scale. With an incentive to produce PEMFC-grade hydrogen, CO was further abated below 1000 ppm by an external PROX in tandem with the fuel processor.

Further studies are highly needed, such as the modification of both catalyst and reformer configurations, taking the thermal conduction into consideration throughout the fuel processor and better management of mass and heat. In addition, a comprehensive numerical simulation will conduce to better understanding the complex interactions among all the parameters and be crucial for future design. Once the key components are implemented, the system currently at a proof-of-concept stage will be ready for transition to a pilot-scale apparatus.

Acknowledgements

The authors thank to SINOPEC for the financial support of this research under contract of 19602. The authors also thank

Shujuan Wang, Shiying Li, Xiuzhen Li and Xiaojie Lou for helping operate the fuel processing system.

References

[1] H. Aki, S. Yamamoto, J. Kondoh, et al., Int. J. Hydrogen Energy 31 (2006) 967–980.
[2] A.F. Ibarreta, C.J. Sung, Int. J. Hydrogen Energy 31 (2006) 1066–1078.
[3] S. Ahmed, M. Krumpelt, Int. J. Hydrogen Energy 26 (2001) 291–301.
[4] F. Joensen, J.R. Rostrup-Nielson, J. Power Sources 105 (2002) 195–201.
[5] D.G. Loffler, K. Taylor, D. Mason, J. Power Sources 117 (2003) 84–91.
[6] Y.S. Seo, A. Shirley, S.T. Kolaczkowski, J. Power Sources 108 (2002) 213–225.
[7] A. Ersoz, H. Olgun, S. Ozdogan, C. Gungor, F. Akgun, M. Tiris, J. Power Sources 118 (2003) 384–392.
[8] B.F. Hagh, J. Power Sources 130 (2004) 85–94.
[9] D.J. Moon, K. Sreekumar, S.D. Lee, B.G. Lee, H.S. Kim, Appl. Catal. A: Gen. 215 (2001) 1–9.
[10] M. Pacheco, J. Sira, J. Kopasz, Appl. Catal. A: Gen. 250 (2003) 161–175.
[11] T.A. Semelsberger, L.F. Brown, R.L. Borup, Int. J. Hydrogen Energy 29 (2004) 1047–1064.
[12] B.F. Hagh, Int. J. Hydrogen Energy 28 (2003) 1369–1377.
[13] A.F. Ibarreta, C.J. Sung, Int. J. Hydrogen Energy 31 (2006) 1066–1078.
[14] D.L. Hoang, S.H. Chan, Appl. Catal. A: Gen. 268 (2004) 207–216.
[15] P.K. Cheekatamarla, A.M. Lane, J. Power Sources 153 (2006) 157–164.
[16] J. Mathiak, A. Heinzel, J. Roes, et al., J. Power Sources 131 (2004) 112–119.
[17] D.G. Loffler, K. Taylor, D. Mason, J. Power Sources 117 (2003) 84.
[18] R.R. Lesieur, T.J. Corrigan, US Patent 6203587B1 (20 March 2001).
[19] P. Irving, Q. Ming, J. Harrison, DOE Hydrogen Program, FY2004 Progress Report, p. 32.
[20] S. Ahmed, R.K. Ahluwalia, S.H. Lee, et al., Proceedings of the Fuel Cell Seminar, San Antonio, 2004.
[21] J.M. Bentley, W.L. Mitchell, L.G. Clawson, J.C. Cross, US Patent 6783742B2 (31 August 2004).
[22] R. Isogawa, Y. Nobata, M. Kondo, et al., US Patent 6390030B1 (21May 2002).
[23] C. Severin, S. Pischinger, J. Ogrzewalla, J. Power Sources 145 (2005) 675–682.
[24] P. Ji, H.J. van der Kooi, J. de Swaan Arons, Chem. Eng. Sci. 58 (2003) 2921.
[25] S.D. Burch, S.G. Goebel, W.H. Pettit, US 6805721B2 (19 October 2004).
[26] E.D. Doss, R. Kumar, R.K. Ahluwalia, M. Krumpelt, J. Power Sources 102 (2001) 1.
[27] D.J. Moon, K. Sreekumar, S.D. Lee, et al., Appl. Catal. A: Gen. 215 (2001) 1–9.
[28] S.S. Sandhu, Y.A. Saif, J.P. Fellner, J. Power Sources 140 (2005) 88–102.
[29] S.-T. Lin, Y.-H. Chen, C.-C. Yu, et al., J. Power Sources 148 (2005) 43–53.
[30] S. Ahmed, R. Ahluwalia, S.H.D. Lee, S. Lottes, J. Power Sources 154 (2006) 214–222.
[31] A. Qi, S. Wang, G. Fu, et al., Appl. Catal. A: Gen. 293 (2005) 71–82.
[32] S.H.D. Lee, D.V. Applegate, S. Ahmed, et al., Int. J. Hydrogen Energy 30 (2005) 829–842.
[33] A. Qi, S. Wang, G. Fu, et al., Appl. Catal. A: Gen. 281 (2005) 233–246.
[34] M. Inbody, R. Borup, J. Hedstrom, et al., Fuel Cell Power Systems, FY 2000 Progress Report, H. CO Clean-Up Development, 2000, pp. 58–62.
[35] P.V. Snytnikov, V.A. Sobyanin, V.D. Belyaev, et al., Appl. Catal. A: Gen. 239 (2003) 149–156.
[36] M.M. Slinko, V.N. Korchak, N.V. Peskov, Appl. Catal. A: Gen. 303 (2006) 258–267.
[37] B.S. Çağlayan, A.K. Avcı, Z.İ. Önsan, A.E. Aksoylu, Appl. Catal. A: Gen. 280 (2005) 181–188.
[38] J.M. Bae, S. Ahmed, R. Kmar, E. Doss, J. Power Sources 139 (2005) 91–95.
[39] M. Pacheco, J. Sira, J. Kopasz, Appl. Catal. A: Gen. 250 (2003) 161–175.
[40] C. Caners, Master's Thesis, Queen's University, 2005.
[41] S. Ahmed, S.H.D. Lee, E. Doss, C. Pereira, D. Colombo, M. Krumpelt, Fuel Cell Power Systems, FY 2000 Progress Report, D. Integrated Fuel Processor Development, 2000, pp. 40–43.
[42] C. Song, Catal. Today 86 (2003) 211–263.
[43] S. Ricote, G. Jacobs, M. Milling, et al., Appl. Catal. A: Gen. 303 (2006) 35–47.